Chemistry of C-Trimethylsilyl-Substituted Stannacarboranes. 2. Synthesis, Characterization, and Tin-119 Mössbauer Effect Study of η^3-Stannaborallyl Complexes of 2,2′-Bipyridine and Tetrahydrofuran. Crystal Structures of 1-Sn-2-[$Si(CH_3)_3$]-2,3-$C_2B_4H_5$ and 1-Sn[$C_{10}H_8N_2$]-2,3-[$Si(CH_3)_3$]$_2$-2,3-$C_2B_4H_4$

Narayan S. Hosmane,* Patrice de Meester, Noormahmad N. Maldar, Stephen B. Potts, and Shirley S. C. Chu

Departments of Chemistry, and Electrical Engineering, Southern Methodist University, Dallas, Texas 75275

Rolfe H. Herber

Department of Chemistry, Rutgers, The State University, New Brunswick, New Jersey 08903

Received August 5, 1985

The stannacarboranes $Sn[Si(CH_3)_3]_2C_2B_4H_4$ (I), $Sn[Si(CH_3)_3][CH_3]C_2B_4H_4$ (II), and $Sn[Si(CH_3)_3]C_2B_4H_5$ (III) react quantitatively with 2,2′-bipyridine in benzene to form the electron acceptor–donor complexes $[C_{10}H_8N_2]Sn[Si(CH_3)_3]_2C_2B_4H_4$ (IV), $[C_{10}H_8N_2]Sn[Si(CH_3)_3][CH_3]C_2B_4H_4$ (V), and $[C_{10}H_8N_2]Sn[Si(CH_3)_3]C_2B_4H_5$ (VI), respectively. The structures of III and IV were determined by single-crystal X-ray diffraction. The ^{119m}Sn Mössbauer effect spectra of these complexes exhibit quadrupole split doublets and clearly indicate that tin is formally in the tin(II) oxidation state. The fact that a bipyridyl donor group on the opposite side of the five-membered carborane ring appears to have so little effect on the Mössbauer parameters of the tin atom is unexpected. The infrared spectra, mass spectra, ^{1}H, ^{11}B, ^{13}C, ^{29}Si, and ^{119}Sn NMR, and ^{119m}Sn Mössbauer spectra of IV, V, and VI are all consistent with the crystal structure of IV, having a distorted pentagonal-bipyramidal geometry with the tin atom occupying an apical position and bonding exclusively to the three boron atoms of the carborane ring and two nitrogen atoms of the bipyridine ring on the opposite side. The NMR spectra show evidence for the formation of air-sensitive THF–stannacarborane complex intermediates $[C_4H_8O]_2Sn[Si(CH_3)_3]_2C_2B_4H_4$ (VII), $[C_4H_8O]_2Sn[Si(CH_3)_3][CH_3]C_2B_4H_4$ (VIII), and $[C_4H_8O]_2Sn[Si(CH_3)_3]C_2B_4H_5$ (IX), which readily decompose to give THF and the stannacarboranes I, II, and III, respectively. Compound III crystallizes in the monoclinic space group $C2/c$ with a = 19.453 (4) Å, b = 20.728 (7) Å, c = 6.519 (2) Å, β = 122.89 (2)°, U = 2207.3 (1.1) Å^3, and Z = 8. Full-matrix least-squares refinement converged at R = 0.026 and R_w = 0.028. Compound IV crystallizes in the monoclinic space group $P2_1/c$ with a = 19.703 (4) Å, b = 9.724 (2) Å, c = 14.939 (2) Å, β = 119.34 (1)°, U = 2494.9 (8) Å^3, and Z = 4. The structure was refined to R = 0.056 and R_w = 0.063.

Introduction

The recent synthetic and structural investigations of Zuckerman et al.[1] and theoretical calculations of Cowley et al.[2] showed that the tin atom in stannocene fails to form electron donor–acceptor complexes with Lewis acids such as BF_3. A similar trend in stannacarboranes was also observed in our laboratory[3] and elsewhere.[4] In our recent preliminary communication,[5] it has been confirmed that the apical "bare" tin atom of the polyhedral stannacarborane behaves as a Lewis acid despite the presence of a lone pair of electrons[3] and forms electron acceptor–donor complexes with 2,2′-bipyridine. Here we describe, in detail, the preparation, characterization, and ^{119m}Sn Mössbauer study of 2,2′-bipyridine complexes of C-trimethylsilyl-substituted stannacarboranes, in addition to the crystal structures of *closo*-1-Sn-2-(Me_3Si)-2,3-$C_2B_4H_5$ (III) and 1-Sn(bipyridyl)-2,3-(Me_3Si)$_2$-2,3-$C_2B_4H_4$ (IV). We also show spectroscopic evidence for the formation of an unstable complex intermediate, THF–stannacarborane, during the preparation of stannacarboranes I, II, and III.

Results and Discussion

Synthesis. Recently we have reported[3] that the failure of stannacarboranes $Sn(Me_3Si)_2C_2B_4H_4$ (I), $Sn(Me_3Si)(Me)C_2B_4H_4$ (II), and $Sn(Me_3Si)C_2B_4H_5$ (III) to form electron donor complexes with BF_3 or BH_3 is in line with the interpretation that the exo-polyhedral lone pair of electrons on the tin atom is diffuse, with relatively little directional character. However, I, II, and III reacted instantaneously with 2,2′-bipyridine in benzene to form electron acceptor–donor complexes $(C_{10}H_8N_2)Sn(Me_3Si)_2C_2B_4H_4$ (IV), $(C_{10}H_8N_2)Sn(Me_3Si)(Me)C_2B_4H_4$ (V), and $(C_{10}H_8N_2)Sn(Me_3Si)C_2B_4H_5$ (VI), (see Experimental Section). This suggests that the apical "bare" tin atom of the stannacarboranes is behaving as a Lewis acid as in the case of the pyridine or bipyridine complexes of $[(Me_5C_5)Sn^+]$.[6]

The reinvestigation of syntheses of I, II, and III indicated that there is a formation of an unstable intermediate, a red THF complex, which upon heating or even at room

(1) (a) Dory, T. S.; Zuckerman, J. J.; Barnes, C. L. *J. Organomet. Chem.* **1985**, *281*, C1. (b) Dory, T. S.; Zuckerman, J. J.; Rausch, M. D. *J. Organomet. Chem.* **1985**, *281*, C8.

(2) Baxter, S. G.; Cowley, A. H.; Lasch, J. G.; Lattman, M.; Sharnn, W. P.; Stewart, C. A. *J. Am. Chem. Soc.* **1982**, *104*, 4064.

(3) Hosmane, N. S.; Sirmokadam, N. N.; Herber, R. H. *Organometallics* **1984**, *3*, 1665.

(4) (a) Rudolph, R. W.; Voorhees, R. L.; Cochoy, R. E. *J. Am. Chem. Soc.* **1970**, *92*, 3351. (b) Voorhees, R. L.; Rudolph, R. W. *Ibid.* **1969**, *91*, 2173. (c) Chowdhry, V.; Pretzer, W. R.; Rai, D. N.; Rudolph, R. W. *Ibid.* **1973**, *95*, 4560.

(5) Cowley, A. H.; Galow, P.; Hosmane, N. S.; Jutzi, P.; Norman, N. C. *J. Chem. Soc., Chem. Commun.* **1984**, 1564.

(6) (a) Jutzi, P.; Kohl, F.; Kruger, C. *Angew. Chem., Int. Ed. Engl.* **1979**, *18*, 59. (b) Jutzi, P.; Kohl, F.; Hofmann, P.; Kruger, C.; Tsay, Y.-H. *Chem. Ber.* **1980**, *113*, 757. (c) Kohl, F. X.; Jutzi, P. *Ibid.* **1981**, *114*, 488.

0276-7333/86/2305-0772$01.50/0

Table I. Summary of ^{119m}Sn Mössbauer Data

sample	IV	V	VI
IS (78 K),[b] mm s^{-1}	3.102 ± 0.012	2.963 ± 0.004	2.923 ± 0.007
QS (78 K), mm s^{-1}	2.726 ± 0.028	3.012 ± 0.012	2.970 ± 0.019
d(ln A)/dT, K^{-1}	1.85 × 10^{-2}	1.87 × 10^{-2}	1.67 × 10^{-2}
Γ, mm s^{-1}	0.85 ± 0.03	0.85 ± 0.03	0.86 ± 0.10[a]
T range, K	78–120	78–130	78–140

[a] The larger experimental errors associated with this sample arise from the presence of a tin-containing impurity (IS ≈ 1 mm s^{-1}) associated with partial oxidation of the subject compound. [b] With respect to $CaSnO_3$ at 295 K.

temperature in vacuo evolves THF and corresponding stannacarborane quantitatively as shown in eq 1 and hence confirms the Lewis acidity of the tin atom. These facts further support the ease of electron pair acceptance by I, II, and III.

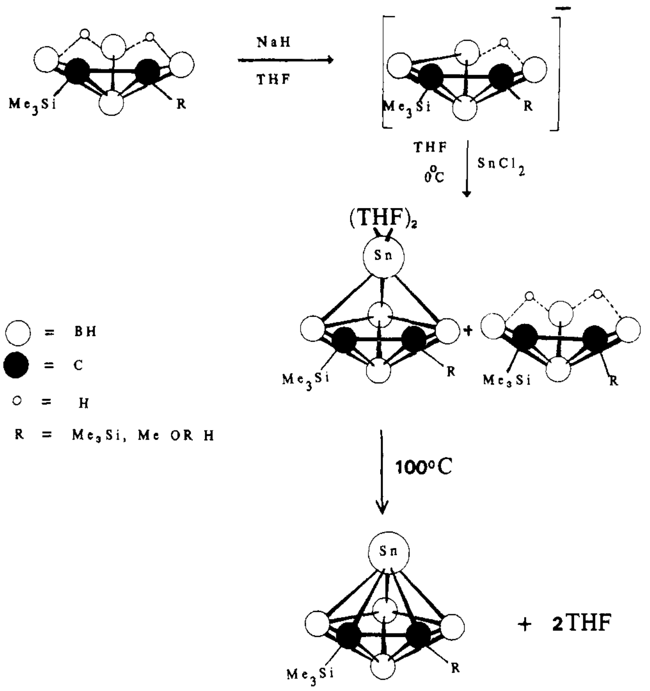

(1)

When pure stannacarboranes I, II, and III were allowed to react with THF, the complexes VII, VIII, and IX formed, respectively, in very small quantities, over a long period of time. Therefore, it is reasonable to assume that the THF–stannacarborane complex forms during the preparation of I, II, or III much earlier than the formation of same complex from the stannacarborane itself. These reactions are shown in eq 2–4.

$$SnCl_2 + 2THF \rightarrow (THF)_2SnCl_2 \quad (2)$$

$$(THF)_2SnCl_2 + Na^+[(Me_3Si)(R)C_2B_4H_5]^- \xrightarrow{0\ °C} NaCl + (THF)_2Sn(Me_3Si)(R)C_2B_4H_4 + HCl \quad (3)$$

$$2(THF)_2Sn(Me_3Si)(R)C_2B_4H_4 + 2HCl \rightarrow (THF)_2SnCl_2 + (Me_3Si)(R)C_2B_4H_6 + (THF)_2Sn(Me_3Si)(R)C_2B_4H_4 \quad (4)$$

NMR Spectra. The bipyridine complexes IV, V, and VI were characterized from their ^{1}H, ^{11}B, ^{13}C, ^{29}Si, and ^{119}Sn pulse Fourier transform NMR, IR, and mass spectra, elemental analysis, and ^{119m}Sn Mössbauer studies (Experimental Section and Table I).

The ^{1}H NMR and ^{13}C NMR spectra clearly indicate the presence of a bipyridine ring in IV, V, and VI in addition to the $SiMe_3$ and Me or CH groups, respectively. Since ^{13}C chemical shifts of the cage carbons were not changed significantly,[7] it may be interpreted that the interaction between cage carbon atoms and the tin atom is minimum. This is further confirmed by the crystal structure of IV (discussed in the following section) where the tin atom is exclusively bonded to three boron atoms. Except for the small shift of the apical ^{11}B resonance, due to less interaction with the tin atom, the ^{11}B NMR data of IV, V, and VI bear striking similarities to those of I, II, and III. The most significant features in the ^{11}B NMR spectra are that the basal B–H (terminal) coupling values are significantly less than those of the corresponding stannacarborane precursors I, II, and III. The broad resonances in the ^{119}Sn NMR spectra of the complexes appear at different chemical shifts, and the values are less negative than those of stannacarborane precursors. This is not at all surprising when tin is bonded to donor atoms such as nitrogens which could effectively shield the metal atom. The ^{29}Si NMR spectra of IV, V, and VI are not significantly different from those of many carborane compounds which we have studied so far.[3,7,8]

The THF complexes $(THF)_2Sn(Me_3Si)_2C_2B_4H_4$ (VII), $(THF)_2Sn(Me_3Si)(Me)C_2B_4H_4$ (VIII), and $(THF)_2Sn(Me_3Si)C_2B_4H_5$ (IX) were characterized by ^{1}H, ^{11}B, ^{13}C, ^{29}Si, and ^{119}Sn pulse Fourier transform NMR spectroscopy (see Experimental Section). The most significant features in the ^{119}Sn NMR spectra are the chemical shift of the broad peaks which are more negative than those of stannacarboranes I, II, and III, due to the coordination of the electronegative oxygen atom to the tin atom. X-ray quality crystals of VII, VIII, and IX have not yet been obtained. All attempts to obtain the elemental analyses and mass and infrared spectra for these complexes failed due to their extreme air sensitivity and thermal instability, even at room temperature. However, the NMR data of these THF–stannacarborane complexes are all consistent with the proposed structure shown in eq 1. The structures of these complexes may very well be similar to those of bipyridine complexes IV, V, and VI.

Mass Spectra. The electron-impact (EI) mass spectra of IV and VI (Table 4 (supplementary material)) do not exhibit the parent ions. However, the EI mass spectrum of V exhibited a weak parent grouping $[(^{12}C_{10}H_8{}^{14}N_2)^{120}Sn(^{12}CH_3)_4{}^{28}Si^{12}C_2{}^{11}B_4H_4{}^+]$ with the major cutoff at m/z 436. The most common ion fragments for all these complexes appear at m/z 45, 59, 73, 78, and 156, as intense peaks, corresponding to $^{12}CH_3{}^{28}SiH_2{}^+$, $(^{12}CH_3)_2{}^{28}SiH^+$, $(^{12}CH_3)_3Si^+$, $^{12}C_5H_4{}^{14}N^+$, and $^{12}C_{10}H_8{}^{14}N_2{}^+$, respectively. The groupings with the major cutoffs at m/z are 338 and 323 for IV corresponding to the fragments $^{120}Sn(^{12}CH_3)_6{}^{28}Si_2{}^{12}C_2{}^{11}B_4H_4{}^+$ and $^{120}Sn(^{12}CH_3)_5{}^{28}Si_2{}^{12}C_2{}^{11}B_4H_4{}^+$, 280 and 265 for V corresponding to $^{120}Sn(^{12}CH_3)_4{}^{28}Si^{12}C_2{}^{11}B_4H_4{}^+$ and $^{120}Sn(^{12}CH_3)_3{}^{28}Si^{12}C_2{}^{11}B_4H_4{}^+$, and 266 and 251 for VI corresponding to $^{120}Sn(^{12}CH_3)_3{}^{28}Si^{12}C_2{}^{11}B_4H_5{}^+$ and $^{120}Sn(^{12}CH_3)_2{}^{28}Si^{12}C_2{}^{11}B_4H_5{}^+$.

The absence of the parent ion and the presence of bipyridine ion fragment with 100% relative intensity, in the EI mass spectra of IV and VI, indicate that the Sn–N bonds in those complexes are very weak; consequently, these bonds were ruptured during the ionization at 70 eV. It was also observed that the most intense peaks were not

(7) The ^{13}C chemical shift of the cage carbons in $Os(CO)_3(Me_3Si)_2C_2B_4H_4$ appear as a broad singlet at 89.93 ppm due to the π bonding between cage carbons and osmium metal: Hosmane, N. S.; Sirmokadam, N. N. *Organometallics* **1984**, *3*, 1119.

(8) (a) Hosmane, N. S.; Cradock, S.; Ebsworth, E. A. V. *Inorg. Chim. Acta* **1983**, *72*, 181. (b) Hosmane, N. S.; Dehghan, M.; Davies, S. *J. Am. Chem. Soc.* **1984**, *106*, 6435. (c) Hosmane, N. S.; Sirmokadam, N. N.; Mollenhauer, M. N. *J. Organomet. Chem.* **1985**, *279*, 359. (d) Hosmane, N. S.; Mollenhauer, M. N.; Cowley, A. H.; Norman, N. C. *Organometallics* **1985**, *4*, 1194.

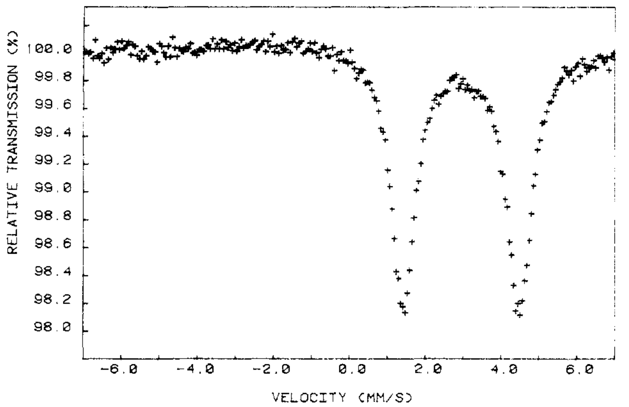

Figure 1. ^{119m}Sn Mössbauer spectrum of V at 78 K.

in the region of the daughter ion but in the region of the daughter ion minus one methyl group. This phenomenon was also observed elsewhere.[9]

Mössbauer Effect Study and Vibrational Spectroscopy of $(C_{10}H_8N_2)Sn(Me_3Si)(R)C_2B_4H_4$ Derivatives (R = Me_3Si, Me, or H). The ^{119m}Sn Mössbauer effect data are summarized in Table I, and a representative spectrum is shown in Figure 1. All three compounds yield spectra at liquid-nitrogen temperature which consist of two resonance maxima with isomer shifts (relative to a room-temperature spectrum of $CaSnO_3$) of ~3 mm s^{-1}, and the tin atom can be formally assigned a stannous charge state. The differences between the observed isomer shifts and those associated with an essentially "bare" Sn^{2+} configuration are a consequence of the covalent contributions[10] to the Sn–B bonding interaction as well as the covalency in the tin–nitrogen bond to the bipyridyl moiety. The observed isomer shifts at 78 K are ~0.2 mm s^{-1} smaller than those which have been reported earlier[3] for the stannacarborane precursors.

The observed quadrupole hyperfine interactions arise primarily from the lone pair on the metal atom and are of the same order of magnitude as those reported in the earlier study.[3] As in the case of the stannacarboranes, there is no noticeable correlation between the magnitude of the quadrupole splitting and the nature of the substituents on the two carbon atoms of the cage structure, suggesting that both direct σ framework electronic effects and steric hindrance effects due to these C-bonded groups are negligible, despite the presence of the bulky bipyridyl group bonded to the metal atom.

The temperature dependence of the ^{119}Sn recoil-free fraction is identical (within experimental error) in IV and V and ~ 10% smaller than in the precursor stannacarboranes, presumably due to the presence of the bipyridyl group proximal to the metal atom, which would be expected to reduce the mean square amplitude of the thermally driven tin atom motion.

The band positions of a number of significant infrared absorptions are summarized in Table S5A (supplementary material). The most significant difference between IV and V is to be noted in the BH stretching region; in the former there are three bands resolved from the data while in V there are only two bands noted in the range 2600–2400 cm^{-1}. These bands show a small (~3 cm^{-1}) blue shift between liquid nitrogen and room temperature, but the bands are not sufficiently sharp to permit a correlation between this temperature dependence and possible structural changes over this temperature interval. The cage carborane bending mode region at ~630 cm^{-1} and the Sn–N stretching and a ring breathing mode region[11] at ~1245 cm^{-1} are very similar in both IV and V, in consonance with the identity of the bonding environment around the metal atom in the two compounds as discussed above. None of these bands show a pronounced temperature dependence of either the band positions or intensities, and it may thus be safely inferred that there are no significant structural changes in these solids between the two temperature limits. Consequently, the low-temperature ^{119m}Sn Mössbauer effect data pertain to the same molecular configurations as the room-temperature single-crystal X-ray diffraction data which are cited in detail, and the various spectroscopic techniques employed to characterize these compounds provide a consistent view of the subject stannacarborane complexes.

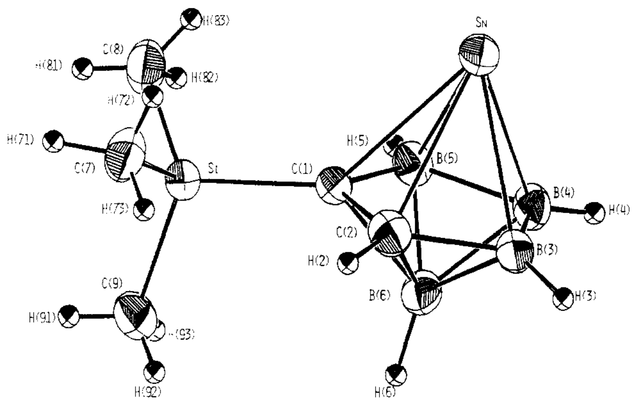

Figure 2. ORTEP view of $Sn(Me_3Si)C_2B_4H_5$ (III) showing the atom numbering scheme and thermal ellipsoids at the 50% probability level. Hydrogen atoms are represented by small spheres of arbitrary radii.

Crystal Structures of $Sn(Me_3Si)C_2B_4H_5$ (III) and $(C_{10}H_8N_2)Sn(Me_3Si)_2C_2B_4H_4$ (IV). The X-ray molecular structure of III, represented in Figure 2, shows that the Sn atom at the apex of a distorted pentagonal bipyramid is essentially η^5 bonded to the C_2B_3 face. This distortion involves primarily the Sn–C distances [2.518 (5) and 2.475 (6) Å], which are slightly but significantly longer than the Sn–B distances [2.397 (8), 2.432 (7), and 2.431 (7) Å], thus confirming the NMR evidence[3] for such an elongation. Very similar distances were found in II, where the hydrogen atom is replaced by a methyl group on cage carbon C(2).[5] One of the few examples which can directly be compared to III is 1-$MeGaC_2B_4H_6$,[12] where the Ga–C distances were found to be ca. 0.1 Å longer than the Ga–B distances. It may also be noted that in these compounds, the shortest of the five metal–C_2B_3 bonds involves the boron atom opposite to the cage C–C bond. But this is probably just a consequence of geometry (i.e., not electronic).

When the 2,2′-bipyridyl group is bonded to Sn as in IV (see Figure 3), the metal atom is still involved in five short bonds, two Sn–N bonds of lengths 2.49 (1) and 2.52 (1) Å and the three Sn–B distances that remain essentially unchanged when compared to those in III. As a consequence of the formation of Sn–N bonds, the Sn–C distances undergo a substantial elongation [2.70 (1) and 2.75 (1) Å]. Therefore, the Sn atom may be viewed as interacting only

(9) (a) Hobrock, B. G.; Koser, R. W. *J. Phys. Chem.* **1962**, *66*, 155. (b) Dibeler, V. H. *J. Res. Natl. Bur. Stand. (U.S.)* **1952**, *49*, 235 and references therein. (c) Gaines, D. F.; Iorns, T. V. *J. Am. Chem. Soc.* **1968**, *90*, 6617.

(10) (a) Rudolph, R. W.; Chowdhry, V. *Inorg. Chem.* **1974**, *13*, 248. (b) Herber, R. H.; Carrasquillo, G. *Inorg. Chem.* **1981**, *20*, 3693.

(11) Bishop, M. E. Zuckerman, J. J. *Inorg. Chem.* **1977**, *16*, 1749.

(12) Grimes, R. N.; Rademaker, W. J.; Denniston, M. L.; Bryan, R. F.; Greene, P. T. *J. Am. Chem. Soc.* **1972**, *94*, 1865.

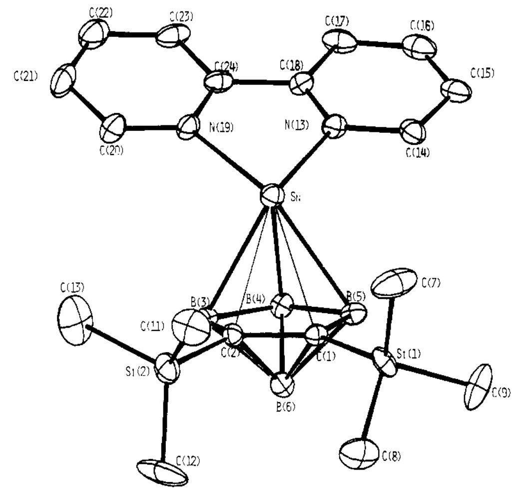

Figure 3. Front view of $(C_{10}H_8N_2)Sn(Me_3Si)_2C_2B_4H_4$ (IV), with thermal ellipsoids drawn at 20% probability level. The thinner lines represent weaker interactions between Sn and cage carbons.

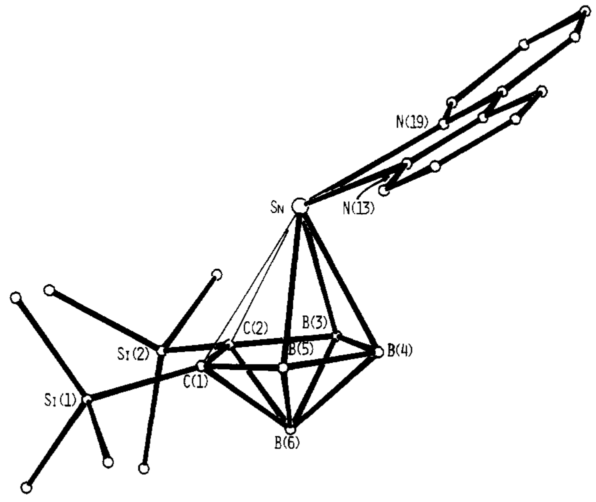

Figure 4. A side view of IV.

weakly with the cage carbon atoms. The slippage of the Sn atom relative to the pentagonal face is less important in IV than that observed in $(C_{10}H_8N_2)Sn(Me)_2C_2B_9H_9$ (X).[5] A number of reported metallacarborane structures show diverse degrees of slippage of the metal atom relative to the bonded cage.[13]

It is best seen in Figure 4 that the bipyridyl group has a particular orientation, away from the C(1) and C(2) atoms. It may be that this is simply due to steric effects imposed by the bulky trimethylsilyl groups bonded to these two carbon atoms. However, when both these carbon atoms carry only methyl groups as in X, the bipyridyl group still adopts the same position.

Summary. It is clear that there is a distortion from η^5 toward η^3 bonding in IV as in the case of X. The crystal structures of both of these complexes unambiguously confirm that the bonding of Sn is exclusively to the three boron atoms: consequently, the complexes IV–VI and VII–X all can be regarded at η^3-stannaborallyl complexes.

Experimental Section

Materials. 2,3-Bis(trimethylsilyl)-2,3-dicarba-*nido*-hexaborane(8), 2-(trimethylsilyl)-3-methyl-2,3-dicarba-*nido*-hexaborane(8), and 2-(trimethylsilyl)-2,3-dicarba-*nido*-hexaborane(8) were prepared by the methods of Hosmane et al.[14] 1-Stanna-2,3-bis(trimethylsilyl)-2,3-dicarba-*closo*-heptaborane(6), 1-stanna-2-(trimethylsilyl)-3-methyl-2,3-dicarba-*closo*-heptaborane(6), and 1-stanna-2-(trimethylsilyl)-2,3-dicarba-*closo*-heptaborane(6) were prepared by using methods described elsewhere.[3] Solutions of the sodium salts of *nido*-carborane anions, $Na^+[C\text{-}Si(CH_3)_3\text{-}C'\text{-}R\text{-}2,3\text{-}C_2B_4H_5]^-$ (R = $Si(CH_3)_3$, CH_3, or H), in THF were prepared by the method of Onak and Dunks.[15] Anhydrous tin(II) chloride was obtained from Johnson Matthey, Inc., Seabrook, NH, and used without further purification. 2,2′-Bipyridine was obtained from Aldrich Chemical Co., Milwaukee, WI, and sublimed in vacuo before use. THF and benzene were dried over $LiAlH_4$ and double distilled before use. All other solvents were dried over 4–8 mesh molecular sieve (Davidson) and either saturated with dry argon or degassed before use.

Spectroscopic Procedures. Proton, boron-11, carbon-13, silicon-29, and tin-119 pulse Fourier transform NMR spectra, at 200, 64.2, 50.3, 39.76, and 74.63 MHz, respectively, were recorded on an IBM-200SY multinuclear NMR spectrometer. Mass spectral data were obtained on a Hewlett-Packard GC/MS system 5988A and at Cornell University[16] by using an AEI MS 902/CI S-2 VG data no. system 2040. Infrared spectra were obtained by using both dispersive and Fourier transform spectrometers. The former were run on a Perkin-Elmer Model 283 microprocessor controlled instrument, and the latter were acquired on an IBM Model 32 nitrogen-purged spectrometer in which 100–200 scans were taken at 2 cm^{-1} resolution. FT-IR spectra were recorded at both room temperature and 78 K, using an Invar sample cell mounted on the cold end of a Heli-tran cryostat[17] as described earlier.[18] All samples were prepared as 0.5–1% w/w solutes in KBr, and the spectra were ratioed to a KBr pellet background. ^{119m}Sn Mössbauer spectra were obtained in the temperature range $78 \leq T \leq 160$ K by using the constant-acceleration spectrometer described earlier.[3,19] Spectrometer calibration was effected by using NBS SRM 0.85 mil iron foil and the magnetic hyperfine splitting data of Spijkerman et al.[20] Data reduction was carried out by using the SPECTRA program of Trooster and Viegers[21] modified to run on the Rutgers NAS-9000 computer. All isomer shifts are reported with respect to a reference spectrum of $CaSnO_3$ at 295 K obtained by using the same ^{119m}Sn Mössbauer source. All samples were examined as powders in high purity aluminum foil thermally clamped to copper sample holders mounted in a cryostat.[3,19] Elemental analyses were obtained from Galbraith Laboratories, Knoxville, TN.

X-ray Analysis of III and IV. Large well-formed clear colorless crystals of III and orange crystals of IV were grown by sublimation onto a glass surface. Preliminary experiments indicated that both compounds were sensitive not only to air but also to X-rays. They were coated in an epoxy resin and mounted on an automatic Syntex $P2_1$ diffractometer, approximately along the *c* axis for III and the *b* axis for IV. Unit-cell dimensions were refined by least-squares fit of 15 reflections measured in the range $15 < 2\theta < 26°$ for III and $19 < 2\theta < 24°$ for IV.

Systematic absences were consistent with space groups $C2/c$ and Cc for III, the former being assigned from the successful solution and refinement of the structure, and space group $P2_1/c$ for IV. The pertinent crystallographic data are summarized in Table II. Three standard reflections, remeasured after every 100 reflections, showed that both crystals underwent severe decomposition during data collection (ca. 38 h for III and 43 h for IV). Both data sets were processed, rescaled according to the values reached by the standard reflections, and corrected for Lorentz and polarization effects but not for absorption. Only the observed reflections with $I > 3\sigma(I)$ were used in the subsequent solution and refinement of the structures. The structures were solved by

(13) Barker, G. K.; Green, M.; Onak, T. P.; Stone, F. G. A.; Ungermann, C. B.; Welch, A. J. *J. Chem. Soc., Chem. Commun.* **1978**, 169 and references therein.
(14) Reference 8c.
(15) Onak, T.; Dunks, G. B. *Inorg. Chem.* **1966**, *5*, 439.
(16) Cornell Mass Spectrometry Facility, Ithaca, NY 14853. We are indebted to Dr. T. Wachs for running these mass spectra for us.
(17) Air Products Corp., Allentown, PA.
(18) Casson, L. M.; Herber, R. H. *Rev. Sci. Instrum.* **1985**, *56*, 1593. Paper P. 5.11, 1985 International Conference on Fourier and Computerized IR Spectroscopy SPIE, in press.
(19) Rein, A. J.; Herber, R. H. *J. Chem. Phys.* **1975**, *63*, 1021 and references therein.
(20) Spijkerman, J. J.; de Voe, J. R.; Travis, J. C. *NBS Spec. Publ.* (*U.S.*) **1970**, **No. 260-20.**
(21) Trooster, J.; Viegers, T., private communication to R.H.H., 1979.

Table II. Crystallographic Data[a] for III and IV

	III	IV
formula	$C_5H_{14}B_4SiSn$	$C_{18}H_{30}N_2B_4Si_2Sn$
fw	264.17	492.6
cryst system	monoclinic	monoclinic
space group	$C2/c$	$P2_1/c$
a, Å	19.453 (4)	19.703 (4)
b, Å	20.728 (7)	9.724 (2)
c, Å	6.519 (2)	14.939 (2)
β, deg	122.89 (2)	119.34 (1)
U, Å^3	2207.3 (1.1)	2494.9 (8)
Z	8	4
D_{calcd}, g cm^{-3}	1.59	1.311
cryst dimens, mm	0.36 × 0.09 × 0.05	0.61 × 0.30 × 0.06
μ(Mo Kα), cm^{-1}	23.69	11.26
scan type	$\theta/2\theta$	$\theta/2\theta$
scan speed, deg min^{-1}	2.9–14.7	5.9–14.7
2θ range, deg	$3 < 2\theta < 42$	$3 < 2\theta < 40$
data collected	$\pm h,k,l$	$h,k,\pm l$
decay, %	22.1	24.9
unique data	1199	2318
obsd reflctns, $I > 3\sigma(I)$	973	1600
R^b	0.026	0.056
R_w	0.028	0.063
$\Delta\rho$ (max, min), e/Å^3	0.40, −0.48	0.65, −0.45

[a] Graphite-monochromatized Mo Kα radiation, λ = 0.71069 Å. [b] $R = \sum||F_o| - |F_c||/\sum|F_o|$, $R_w = [\sum w(F_o - F_c)^2/\sum(F_o)^2]^{1/2}$, and $w = 1/(\sigma^2(F_o) + kF_o^2)$, where k = 0.0007 for III and 0.0079 for IV.

standard Patterson and difference Fourier methods. Full-matrix least-squares refinements were used throughout, the function minimized being $\sum\omega(F_o - F_c)^2$. All non-hydrogen atoms were allowed to refine anisotropically in both structures. For III, all hydrogen atoms were easily located and subsequently refined isotropically, while for IV, no attempt was made to locate them, owing to the relatively high thermal motion of the trimethylsilyl carbon atoms. In the final stages of refinement, a weighting scheme was used (Table II). The highest residual electron densities were found at ca. 1.1 Å from the Sn atoms in both structures. Calculations were carried out with the SHELX76 system of programs.[22] Scattering factors used for all atoms as well as the real and imaginary parts of the dispersion correction for Sn and Si were those stored in SHELX76. The final atomic coordinates for III and IV are given in Table III. Selected bond lengths and bond angles are presented in Table IV.

Synthetic Procedures. All experiments were carried out in Pyrex glass round-bottom flasks of 250-mL capacity, containing a magnetic stirring bar and fitted with a high vacuum Teflon valve. Nonvolatile substances were manipulated in evacuable glovebags under an atmosphere of dry argon. All known compounds among the products were identified by comparing their infrared and ^{1}H NMR spectra with those of authentic samples.

Synthesis of 1-Sn($C_{10}H_8N_2$)-2-($SiMe_3$)-3-(R)-2,3-$C_2B_4H_4$ (R = $SiMe_3$, Me, and H). $Sn(SiMe_3)_2C_2B_4H_4$ (I) (0.80 g, 2.38 mmol), $Sn(SiMe_3)(Me)C_2B_4H_4$ (II) (0.79 g, 2.82 mmol), or $Sn(SiMe_3)C_2B_4H_5$ (III) (0.55 g, 2.09 mmol) was dissolved in freshly distilled dry benzene (10–15 mL) in vacuo. This solution was then filtered through a frit under high vacuum onto freshly sublimed, anhydrous 2,2′-bipyridine, $C_{10}H_8N_2$ (0.38 g, 2.44 mmol; 0.44 g, 2.82 mmol; or 0.35 g, 2.24 mmol when I, II, or III was used) contained in a 250-mL round-bottom flask maintained at −78 °C. When the reaction flask was placed in an ice bath, a bright orange solid formed immediately, indicating that the reaction is instantaneous. This mixture was constantly stirred for 4 h at 0 °C. No gas evolution was detected during this period. The benzene was then removed by pumping the reaction mixture at room temperature. After removal of all C_6H_6, the reaction flask was heated to 60 °C and pumped through a detachble U-trap at −196 °C over a period of 18 h to remove unreacted 2,2′-bipyridine from the product mixture by mild sublimation. When R = H, 0.11 g, and when R = $SiMe_3$ and Me, only traces of 2,2′-bipyridine were recovered in −196 °C traps. The stannacarborane I, II, or III were not identified in the sublimate. After removal of all the unreacted 2,2′-bipyridine a yellow-orange solid, $(C_{10}H_8N_2)Sn(SiMe_3)_2C_2B_4H_4$ (IV) (1.07 g, 2.17 mmol; 91% yield based on I consumed), $(C_{10}H_8N_2)Sn(SiMe_3)(Me)C_2B_4H_4$ (V) (1.15 g, 2.65 mmol; 94% yield based on II consumed), or $(C_{10}H_8N_2)Sn(SiMe_3)C_2B_4H_5$ (VI) (0.87 g, 2.07 mmol; 99% yield based on III consumed) remained in the reaction flask. The reaction flask was then attached to a U-trap sublimator which was immersed in an ice bath at 0 °C. On heating the yellow-orange solid to 140 °C in vacuo (10^{-6} torr), over a period of 18 h, bright orange needles of IV (1.02 g, 2.07 mmol; 87% yield based on I consumed), V (0.99 g, 2.28 mmol; 81% yield based on II consumed), or VI (0.78 g, 1.86 mmol; 89% yield based on III consumed) were collected on the inside walls of the U-trap. The side arm of the reaction flask and the side arm of the U-trap sublimator were maintained at 140 °C with heating tape during the sublimation.

The physical properties and characterizations of IV are as follows: mp 181–182 °C; reasonably stable in air for a brief period of time; solubility, at room temperature, highly soluble in THF

(22) Sheldrick, G. M. SHELX-76, Programs for Crystal Structure Determination, University of Cambridge, England, 1976.

Table III. Fractional Coordinates of the Hydrogen and Non-Hydrogen Atoms for III and of the Non-Hydrogen Atoms for IV

atom	x	y	z
		III	
Sn	0.1001 (0)	0.1103 (0)	0.1274 (1)
C(1)	0.2341 (3)	0.1215 (2)	0.1570 (9)
C(2)	0.1813 (3)	0.1780 (3)	0.0216 (11)
B(3)	0.1922 (4)	0.0594 (3)	0.0326 (12)
B(4)	0.1041 (4)	0.0771 (4)	−0.2182 (12)
B(5)	0.0978 (4)	0.1564 (3)	−0.2193 (12)
B(6)	0.1900 (4)	0.1207 (3)	−0.1548 (12)
Si	0.3446 (1)	0.1308 (1)	0.4137 (3)
C(7)	0.3561 (5)	0.2054 (4)	0.5858 (14)
C(8)	0.3745 (5)	0.0595 (4)	0.6153 (15)
C(9)	0.4068 (5)	0.1366 (5)	0.2763 (16)
H(2)	0.203 (3)	0.223 (3)	0.065 (10)
H(3)	0.216 (2)	0.023 (2)	0.072 (8)
H(4)	0.068 (3)	0.047 (3)	−0.345 (11)
H(5)	0.058 (3)	0.191 (2)	−0.355 (9)
H(6)	0.226 (3)	0.122 (2)	−0.244 (10)
H(71)	0.406 (3)	0.211 (3)	0.725 (10)
H(72)	0.323 (5)	0.205 (4)	0.635 (14)
H(73)	0.340 (3)	0.243 (3)	0.488 (11)
H(81)	0.422 (4)	0.063 (3)	0.716 (12)
H(82)	0.367 (4)	0.021 (4)	0.529 (12)
H(83)	0.336 (6)	0.043 (6)	0.612 (22)
H(91)	0.455 (5)	0.144 (3)	0.385 (13)
H(92)	0.393 (5)	0.166 (4)	0.171 (15)
H(93)	0.410 (4)	0.094 (3)	0.200 (12)
		IV	
Sn	0.2222 (0)	0.1141 (1)	0.3577 (1)
Si(1)	0.3157 (2)	0.4238 (4)	0.2473 (3)
Si(2)	0.3899 (2)	0.0531 (5)	0.2621 (3)
C(1)	0.2665 (6)	0.2546 (11)	0.2351 (7)
C(2)	0.2925 (7)	0.1144 (10)	0.2418 (8)
B(3)	0.2242 (9)	0.0106 (15)	0.2105 (10)
B(4)	0.1445 (9)	0.0977 (14)	0.1769 (11)
B(5)	0.1757 (7)	0.2619 (14)	0.1998 (9)
B(6)	0.2076 (9)	0.1574 (14)	0.1306 (11)
C(7)	0.3712 (13)	0.4760 (19)	0.3808 (12)
C(8)	0.3711 (12)	0.4362 (20)	0.1766 (15)
C(9)	0.2383 (11)	0.5625 (19)	0.1749 (16)
C(10)	0.4011 (13)	−0.1269 (17)	0.3134 (20)
C(11)	0.4722 (10)	0.1520 (20)	0.3739 (13)
C(12)	0.3978 (13)	0.0694 (34)	0.1481 (15)
N(13)	0.0968 (6)	0.1444 (10)	0.3574 (7)
C(14)	0.0689 (8)	0.2702 (14)	0.3429 (9)
C(15)	0.0019 (9)	0.3016 (16)	0.3479 (9)
C(16)	−0.0367 (8)	0.1958 (21)	0.3639 (9)
C(17)	−0.0094 (8)	0.0621 (16)	0.3779 (9)
C(18)	0.0600 (7)	0.0411 (13)	0.3748 (8)
N(19)	0.1622 (7)	−0.1027 (10)	0.3840 (7)
C(20)	0.2031 (10)	−0.2204 (15)	0.4000 (11)
C(21)	0.1758 (13)	−0.3387 (16)	0.4320 (14)
C(22)	0.1116 (15)	−0.3360 (19)	0.4402 (14)
C(23)	0.0679 (10)	−0.2122 (16)	0.4200 (9)
C(24)	0.0982 (9)	−0.0956 (13)	0.3940 (9)

Table IV. Selected Bond Lengths (Å) and Bond Angles (deg) for III and IV with Standard Deviations in Parentheses

Bond Lengths for III

Sn–C(1)	2.518 (5)	Si–C(8)	1.85 (1)	C(2)–B(6)	1.73 (1)
Sn–C(2)	2.475 (6)	Si–C(9)	1.86 (1)	B(3)–B(4)	1.65 (1)
Sn–B(3)	2.432 (7)	C(1)–C(2)	1.490 (8)	B(3)–B(6)	1.77 (1)
Sn–B(4)	2.397 (8)	C(1)–B(5)	1.504 (9)	B(4)–B(5)	1.64 (1)
Sn–B(5)	2.431 (7)	C(1)–B(6)	1.725 (9)	B(4)–B(6)	1.74 (1)
Si–C(1)	1.885 (6)	C(2)–B(3)	1.59 (1)	B(5)–B(6)	1.75 (1)
Si–C(7)	1.853 (9)				

Bond Angles for III

C(1)–Sn–C(2)	34.7 (2)	B(5)–C(1)–Si	126.1 (4)
C(1)–Sn–B(5)	35.3 (2)	B(6)–C(1)–Si	130.1 (4)
C(2)–Sn–B(3)	37.9 (2)	C(2)–C(1)–B(5)	110.8 (5)
B(3)–Sn–B(4)	39.9 (3)	C(1)–C(2)–B(3)	111.7 (5)
B(4)–Sn–B(5)	39.8 (3)	C(2)–B(3)–B(4)	104.0 (5)
C(1)–Si–C(7)	109.1 (3)	B(3)–B(4)–B(5)	105.2 (6)
C(1)–Si–C(8)	108.4 (3)	C(1)–B(5)–B(4)	108.2 (6)
C(1)–Si–C(9)	107.8 (4)	C(1)–B(6)–C(2)	51.2 (3)
C(7)–Si–C(8)	110.5 (4)	C(1)–B(6)–B(5)	51.3 (4)
C(7)–Si–C(9)	109.9 (4)	C(2)–B(6)–B(3)	54.2 (4)
C(8)–Si–C(9)	111.0 (4)	B(3)–B(6)–B(4)	56.0 (4)
Sn–C(1)–Si	135.4 (3)	B(4)–B(6)–B(5)	56.2 (4)
C(2)–C(1)–Si	122.2 (4)		

Bond Lengths for IV

Sn–C(1)	2.75 (1)	Si(1)–C(8)	1.86 (2)	C(1)–B(6)	1.70 (2)
Sn–C(2)	2.70 (1)	Si(1)–C(9)	1.92 (2)	C(2)–B(3)	1.56 (2)
Sn–B(3)	2.44 (2)	Si(2)–C(2)	1.89 (1)	C(2)–B(6)	1.73 (2)
Sn–B(4)	2.37 (2)	Si(2)–C(10)	1.88 (3)	B(3)–B(4)	1.63 (2)
Sn–B(5)	2.52 (1)	Si(2)–C(11)	1.92 (2)	B(3)–B(6)	1.79 (2)
Sn–N(13)	2.49 (1)	Si(2)–C(12)	1.79 (3)	B(4)–B(5)	1.68 (2)
Sn–N(19)	2.54 (1)	C(1)–C(2)	1.44 (2)	B(4)–B(6)	1.79 (2)
Si(1)–C(1)	1.87 (1)	C(1)–B(5)	1.60 (2)	B(5)–B(6)	1.77 (2)
Si(1)–C(7)	1.81 (2)				

Bond Angles for IV

C(1)–Sn–N(13)	125.4 (3)	Si(1)–C(1)–C(2)	132.4 (9)
C(1)–Sn–N(19)	147.1 (3)	Si(1)–C(1)–B(5)	115.8 (8)
C(2)–Sn–N(13)	145.3 (4)	Si(1)–C(1)–B(6)	131.6 (9)
C(2)–Sn–N(19)	121.7 (4)	Si(2)–C(2)–Sn	134.3 (6)
B(3)–Sn–N(13)	120.2 (4)	Si(2)–C(2)–C(1)	127.5 (9)
B(3)–Sn–N(19)	90.7 (5)	Si(2)–C(2)–B(3)	120.3 (9)
B(4)–Sn–N(13)	85.4 (5)	Si(2)–C(2)–B(6)	131.1 (9)
B(4)–Sn–N(19)	91.8 (5)	C(2)–C(1)–B(5)	112 (1)
B(5)–Sn–N(13)	91.5 (4)	C(1)–C(2)–B(3)	112 (1)
B(5)–Sn–N(19)	129.4 (4)	C(2)–B(3)–B(4)	108 (1)
N(13)–Sn–N(19)	64.0 (4)	B(3)–B(4)–B(5)	103 (1)
C(1)–Sn–C(2)	30.7 (3)	C(1)–B(5)–B(4)	105 (1)
C(1)–Sn–B(5)	35.0 (4)	C(1)–B(6)–C(2)	49.6 (7)
C(2)–Sn–B(3)	34.9 (5)	C(1)–B(6)–B(5)	54.8 (8)
B(3)–Sn–B(4)	39.7 (5)	C(2)–B(6)–B(3)	52.6 (8)
B(4)–Sn–B(5)	40.2 (5)	B(3)–B(6)–B(4)	54.3 (9)
Si(1)–C(1)–Sn	133.7 (5)	B(4)–B(6)–B(5)	56.5 (8)

and acetone and moderately soluble in $CDCl_3$, CCl_4, CH_2Cl_2, or C_6H_6; ^1H NMR (C_6D_6, relative to external Me_4Si) δ 8.68 [d, 2 H, bpy ring, $J(^1H-^1H)$ = 4.5 Hz], 7.59 [d, 2 H, bpy ring, $J(^1H-^1H)$ = 7.3 Hz], 7.02 [t, 2 H, bpy ring, $J(^1H-^1H)$ = 7.4 Hz], 6.59 [t, 2 H, bpy ring, $J(^1H-^1H)$ = 5.9 Hz], 4.97 [q (br), 3 H, basal H_t, $^1J(^1H-^{11}B)$ = 112 Hz], 1.43 [q (br), 1 H, apical H_t, $^1J(^1H-^{11}B)$ = 155 Hz], 0.77 [s, 18 H, $(CH_3)_3Si$]; ^{11}B NMR (THF, relative external $BF_3 \cdot OEt_2$) δ 22.3 [d, 1 B, basal *BH*, $^1J(^{11}B-^1H)$ = 110 Hz], 19.83 [d, 2 B, basal BH, $^1J(^{11}B-^1H)$ = 82 Hz], −21.05 [d, 1 B, apical BH, $^1J(^{11}B-^1H)$ = 162 Hz]; ^{13}C NMR (THF, relative external Me_4Si) δ 152.81 [s, 2,2′-C, bpy ring], 147.77 [d, bpy ring, $^1J(^{13}C-^1H)$ = 183 Hz], 138.60 [d, bpy ring, $^1J(^{13}C-^1H)$ = 168 Hz], 125.02 [d, bpy ring, $^1J(^{13}C-^1H)$ = 165 Hz], 121.83 [d, bpy ring, $^1J(^{13}C-^1H)$ = 164 Hz], 130.25 [s (br), cage carbon], 2.28 [q, $(CH_3)_3Si$, $^1J(^{13}C-^1H)$ = 119 Hz]; ^{29}Si NMR (THF, relative external Me_4Si) δ −6.05 [m (br), $Si(CH_3)_3$, $^2J(^{29}Si-^1H)$ < 3 Hz]; ^{119}Sn NMR (THF, relative external TMT) δ −133.47 [s (br), cage–Sn–bpy]. Anal. Calcd for $C_{18}H_{30}B_4N_2Si_2Sn$: C, 43.89; H, 6.14; N, 5.69; B, 8.78; Si, 11.40; Sn, 24.10. Found: C, 43.22; H, 6.10; N, 5.66; B, 8.47; Si, 10.80; Sn, 24.50.

The physical properties and characterizations of V are as follows: mp 167 °C dec; reasonably stable in air for a short period of time; solubility at 25 °C, highly soluble in THF and acetone and moderately soluble in $CDCl_3$, CCl_4, CH_2Cl_2, or C_6H_6; ^1H NMR (C_6D_6, relative external Me_4Si) δ 8.62 [d, 2 H, bpy ring, $J(^1H-^1H)$ = 3.8 Hz], 8.29 [d, 2 H, bpy ring, $J(^1H-^1H)$ = 8.78 Hz], 7.15 [t, 2 H, bpy ring, $J(^1H-^1H)$ = 7.5 Hz], 6.65 [t, 2 H, bpy ring, $J(^1H-^1H)$ = 5.97 Hz], 4.26 [q (br), 3 H, basal H_t, $^1J(^1H-^{11}B)$ = 105 Hz], 2.99 [s, 3 H, CH_3], 1.63 [q (br), apical H_t, $^1J(^1H-^{11}B)$ = 164 Hz], 0.70 [s, 9 H, $(CH_3)_3Si$]; ^{11}B NMR (THF, relative external $BF_3 \cdot OEt_2$) δ 20.01 [d, 1 B, basal BH, $^1J(^{11}B-^1H)$ = 131 Hz], 15.54 [d, 2 B, basal BH, $^1J(^{11}B-^1H)$ = 108 Hz], −20.15 [d, 1 B, apical BH, $^1J(^{11}B-^1H)$ = 164 Hz]; ^{13}C NMR (THF, relative external Me_4Si) δ 152.47 [s, 2,2′-C, bpy ring], 147.73 [d, bpy ring, $^1J(^{13}C-^1H)$ = 181 Hz], 138.74 [d, bpy ring, $^1J(^{13}C-^1H)$ = 165 Hz], 125.11 [d, bpy ring, $^1J(^{13}C-^1H)$ = 167 Hz], 121.86 [d, bpy ring, $^1J(^{13}C-^1H)$ = 165 Hz], 130.72 [s (br), cage carbon (SiCB)], 123.45 [s (br), cage carbon (CCB)], 23.03 [q, 1 C, CH_3, $^1J(^{13}C-^1H)$ = 127 Hz], 0.97 [q, 3 C, $(CH_3)_3Si$, $^1J(^{13}C-^1H)$ = 120 Hz]; ^{29}Si NMR (THF, relative external Me_4Si) δ −6.27 [m (br), $Si(CH_3)_3$, $^2J(^{29}Si-^1H)$ < 3 Hz]; ^{119}Sn NMR (THF), (relative external TMT) δ −107.8 [s (br), cage–Sn–bipy]. Anal. Calcd for $C_{16}H_{24}B_4N_2SiSn$: C, 44.24; H, 5.569; N, 6.45; B, 9.95; Si, 6.47; Sn, 27.32. Found: C, 43.97; H, 5.42; N, 6.24; B, 9.60; Si, 6.03; Sn, 27.16.

The physical properties and characterizations of VI are as follows: mp 138 °C dec; reasonably stable in air for a brief period of time; solubility, at 25 °C, highly soluble in THF and acetone and moderately soluble in $CDCl_3$, CCl_4, CH_2Cl_2, or C_6H_6; ^1H NMR (C_6D_6, relative external Me_4Si) δ 9.06 [d, 2 H, bpy ring, $J(^1H-^1H)$ = 3.94 Hz], 8.76 [d, 2 H, bpy ring, $J(^1H-^1H)$ = 7.05 Hz], 8.26 [t, 2 H, bpy ring, $J(^1H-^1H)$ = 6.15 Hz], 7.77 [t, 2 H, bpy ring, $J(^1H-^1H)$ = 3.98 Hz], 6.70 [s (br), 1 H, cage CH], 4.05 [q (br), 3 H, basal H_t, ^1J $(^1H-^{11}B)$ = 145 Hz], 1.30 [q (br), 1 H, apical H_t, $^1J(^1H-^{11}B)$ = 166 Hz], 0.05 [s, 9 H, $(CH_3)_3Si$]; ^{11}B NMR (THF, relative external $BF_3 \cdot OEt_2$) δ 21.13 [d, 1 B, basal BH, $^1J(^{11}B-^1H)$ = 146 Hz], 15.07 [d, 2 B, basal BH, $^1J(^{11}B-^1H)$ = 101 Hz], −23.14 [d, 1 B, apical BH, $^1J(^{11}B-^1H)$ = 166 Hz]; ^{13}C NMR (THF, relative external Me_4Si) δ 152.08 [s, 2,2′-C, bpy ring], 147.45 [d, bpy ring, $^1J(^{13}C-^1H)$ = 181 Hz], 139.07 [d, bpy ring, $^1J(^{13}C-^1H)$ = 161 Hz], 125.36 [d, bpy ring, $^1J(^{13}C-^1H)$ = 168 Hz], 121.80 [d, bpy ring, $^1J(^{13}C-^1H)$ = 159 Hz], 129.3 [s (br), cage carbon SiCB], 115.5 [d (br), cage CH, $^1J(^{13}C-^1H)$ = 176 Hz], 2.13 [q, 3 C, $(CH_3)_3Si$, $^1J(^{13}C-^1H)$ = 122 Hz]; ^{29}Si NMR (THF, relative external Me_4Si) δ −4.88 [m (br), $Si(CH_3)_3$, $^2J(^{29}Si-^1H)$ < 3 Hz]; ^{119}Sn NMR (THF, relative external TMT) δ −86.04 [s (br), cage–Sn–bpy]. Anal. Calcd for $C_{15}H_{22}N_2B_4SiSn$: C, 42.86; H, 5.27; N, 6.66; B, 10.29; Si, 6.68; Sn, 28.23. Found: C, 42.45; H, 5.30; N, 6.48; B, 9.58; Si, 6.54; Sn, 28.08.

Synthesis of 1-Sn(THF)$_2$-2-(SiMe$_3$)-3-(R)-2,3-C$_2$B$_4$H$_4$. A THF (100-mL) solution of $Na^+[(Me_3Si)_2C_2B_4H_5]^-$ (5.13 mmol), $Na^+[(Me_3Si)(Me)C_2B_4H_5]^-$ (4.98 mmol), or $Na^+[(Me_3Si)C_2B_4H_6]^-$ (4.91 mmol) was allowed to react with a THF (20 mL) solution of anhydrous $SnCl_2$ (1.14 g, 6.01 mmol; 1.02 g, 5.38 mmol; or 0.99 g, 5.22 mmol) in a procedure identical with that employed in the synthesis of I, II, or III as described elsewhere.[3] After removal of THF and the corresponding neutral *nido*-carborane [0.560 g, 2.55 mmol, of $(Me_3Si)_2C_2B_4H_6$; 0.387 g, 2.39 mmol, of $(Me_3Si)(Me)C_2B_4H_6$; or 0.341 g, 2.30 mmol, of $(Me_3Si)C_2B_4H_7$] the reddish brown residue remaining in the reaction flask was dissolved in $CHCl_3$ (100–150 mL) and filtered through a frit in vacuo. This was repeated 3–4 times to dissolve most of the THF complex among the reaction products. A clear, reddish brown filtrate containing the THF–stannacarborane complex was collected in a 250-mL flask equipped with a Teflon stopcock. The off-white solids NaCl and $SnCl_2$ remained on the frit (not measured) and were discarded. After removal of $CHCl_3$ from the filtrate, a reddish brown residue, $(THF)_2Sn(Me_3Si)_2C_2B_4H_4$ (VII) (0.91 g, 1.89 mmol; 73% yield based on $(Me_3Si)_2C_2B_4H_6$ consumed), $(THF)_2Sn(Me_3Si)(Me)C_2B_4H_4$ (VIII) (0.73 g, 1.73 mmol; 67% yield based on $(Me_3Si)(Me)C_2B_4H_6$ consumed), or $(THF)_2Sn(Me_3Si)C_2B_4H_5$ (IX) (0.69 g, 1.60 mmol); 65% yield based on $(Me_3Si)C_2B_4H_7$ consumed) remained in the flask. This flask was then attached to a U-trap sublimater which was immersed in an ice bath. When the reddish brown residue was heated to 120 °C, in vacuo (10^{-6} torr), over a period of 10 h, THF and corresponding stannacarborane were collected in −196 °C trap and U-trap sublimator at 0 °C, respectively, as sole products. A small quantity of a gray residue (not measured) remained in the flask. However, VII, VIII, or IX was not identified among the products. The quantities and yields of THF and stannacarborane from each complex are as follows: for VII, 0.27 g, of THF (3.75 mmol; 99% yield based on VII consumed) and 0.58 g of I (1.72 mmol; 91% yield based on VII consumed); for VIII, 0.24 g of THF (3.33 mmol; 96% yield based on VIII consumed) and 0.46 g of II (1.65 mmol; 96% yield based on VIII consumed); for IX, 0.24 g of THF (3.33 mmol; 99% yield based on IX consumed) and 0.42 g of III (1.59 mmol; 94% yield based on IX consumed).

In another experiment, pure VII (1.12 mmol), VIII (1.01 mmol), or IX (0.93 mmol) was allowed to stand in a flask, in vacuo, at room temperature. After 24 h, nearly 25% of the complex decomposed to yield stoichiometric quantities of THF and corresponding stannacarborane. This evolution continued for more than 25 days with much slower rate than that observed after 24 h. After 25 days, the total quantities of THF and stannacarborane are as follows: for VII, 1.98 mmol of THF and 0.93 mmol of I; for VIII, 1.95 mmol of THF and 0.94 mmol of II; for IX, 1.70 mmol of THF and 0.71 mmol of III. The NMR samples were freshly prepared and kept frozen in sealed tubes at −196 °C until the spectra were run. The physical properties of VII, VIII, and IX: melting points and elemental analyses could not be obtained since these complexes are extremely sensitive to air and/or moisture. In addition, these complexes are very unstable in solid state at room temperature and are highly soluble in THF but not very soluble in other organic solvents.

Characterization of VII: ^{1}H NMR ($CDCl_3$, relative to external Me_4Si) δ 4.79 [q (br), 3 H, basal H_t, $^1J(^1H-^{11}B)$ = 104 Hz], 3.15 [q (br), 1 H, apical H_t, $^1J(^1H-^{11}B)$ = 144 Hz], 3.82 [s, 8 H, THF], 1.97 [s, 8 H, THF], 0.28 [s, 18 H, $(CH_3)_3Si$]; ^{11}B NMR (THF, relative external $BF_3{\cdot}OEt_2$) δ 22.49 [d, 3 B, basal BH, $^1J(^{11}B-^1H)$ = 106 Hz], −11.03 [d, 1 B, apical BH, $^1J(^{11}B-^1H)$ = 145 Hz]; ^{13}C NMR ($CDCl_3$, relative external Me_4Si) δ 132.21 [s (br), cage carbons], 67.51 [t, THF, $^1J(^{13}C-^1H)$ = 146 Hz], 25.48 [t, THF, $^1J(^{13}C-^1H)$ = 133 Hz], 1.28 [q, $(CH_3)_3Si$, $^1J(^{13}C-^1H)$ = 120 Hz]; ^{29}Si NMR (THF, relative external Me_4Si) δ −4.71 [m (br), $Si(CH_3)_3$, $^2J(^{29}Si-^1H)$ = 4.3 Hz]; ^{119}Sn NMR (THF, relative external TMT) δ −214.61 [s (br), cage–Sn–THF].

Characterization of VIII: ^{1}H NMR ($CDCl_3$, relative to external Me_4Si) δ 3.89 [q (br), 3 H, basal H_t, $^1J(^1H-^{11}B)$ = 136 Hz], 2.93 [q (br), 1 H, apical H_t, $^1J(^1H-^{11}B)$ = 160 Hz], 3.77 [s, 8 H, THF], 2.43 [s, 3 H, CH_3], 1.92 [s, 8 H, THF], 0.24 [s, 9 H, $(CH_3)_3Si$]; ^{11}B NMR (THF), (relative external $BF_3{\cdot}OEt_2$) δ 22.81 [d, 1 B, basal BH, $^1J(^{11}B-^1H)$ = 150 Hz], 17.98 [d, 2 B, basal BH, $^1J(^{11}B-^1H)$ = 134 Hz], −9.29 [d, 1 B, apical BH, $^1J(^{11}B-^1H)$ = 161 Hz]; ^{13}C NMR ($CDCl_3$, relative external Me_4Si) δ 134.34 [s (br), cage carbon (SiCB)], 126.51 [s (br), cage carbon (CCB)], 67.5 [t, THF, $^1J(^{13}C-^1H)$ = 145 Hz], 25.62 [t, THF, $^1J(^{13}C-^1H)$ = 132 Hz], 23.13 [q, 1 C, CH_3, $^1J(^{13}C-^1H)$ = 126 Hz], −0.14 [q, $(CH_3)_3Si$, $^1J(^{13}C-^1H)$ = 119 Hz]; ^{29}Si NMR (THF, relative external Me_4Si) δ −3.91 [m (br), $Si(CH_3)_3$ $^2J(^{29}Si-^1H)$ < 3 Hz]; ^{119}Sn NMR (THF, relative external TMT) δ −198.73 [s (br), cage–Sn–THF].

Characterizations of IX: ^{1}H NMR ($CDCl_3$, relative external Me_4Si) δ 7.04 [s (v br), 1 H, cage CH], 3.98 [q (br), 3 H, basal H_t, $^1J(^1H-^{11}B)$ = 115 Hz], 2.92 [q (br), 1 H, apical H_t, $^1J(^1H-^{11}B)$ = 160 Hz], 3.76 [s, 8 H, THF], 1.91 [s, 8 H, THF], 0.20 [s, 9 H, $(CH_3)_3Si$]; ^{11}B NMR (THF, relative external $BF_3{\cdot}OEt_2$) δ 22.2 [d, 1 B, basal BH, $^1J(^{11}B-^1H)$ = 140 Hz], 16.58 [d, 2 B, basal BH, $^1J(^{11}B-^1H)$ = 118 Hz], −9.89 [d, 1 B, apical BH, $^1J(^{11}B-^1H)$ = 161 Hz]; ^{13}C NMR ($CDCl_3$) (relative external Me_4Si) δ 135.43 [s (br), cage carbon (SiCB)], 126.28 [d (br), cage CH, $^1J(^{13}C-^1H)$ = 174 Hz], 67.48 [t, THF, $^1J(^{13}C-^1H)$ = 146 Hz], 25.57 [t, THF, $^1J(^{13}C-^1H)$ = 132 Hz], 0.61 [q, 3 C, $(CH_3)_3Si$, $^1J(^{13}C-^1H)$ = 118 Hz]; ^{29}Si NMR (THF, relative external Me_4Si) δ −2.74 [m (Br), $Si(CH_3)_3$, $^2J(^{29}Si-^1H)$ = 4.1 Hz]; ^{119}Sn NMR (THF, (relative external TMT) δ −200.7 [s (br), cage–Sn–THF].

Reaction of I, II, or III with THF. In separate experiments, pure I, II, and III were dissolved in large excess of THF (20 mL) in vacuo and the solutions were allowed to stand for several days at 0 °C and further at room temperature until the colorless solutions turned to light reddish brown. The multinuclear NMR spectra of these solutions showed the presence of VII, VIII, and IX in small quantities in addition to the large quantities of starting materials I, II, and III, respectively.

Acknowledgment. This work was supported by grants from the National Science Foundation under Grant No. CHE-84-18874 (N.S.H.), The Robert A. Welch Foundation (N.S.H. and S.S.C.C.), and the donors of the Petroleum Research Fund, administered by the American Chemical Society (N.S.H.). We thank Professor John A. Maguire for helpful suggestions concerning this work. N.N.M. and P.deM. gratefully acknowledge Postdoctoral Fellowships from the Welch Foundation.

Registry No. I, 90388-43-5; II, 91670-63-2; III, 91686-40-7; IV, 100333-68-4; V, 100333-69-5; VI, 100349-86-8; VII, 100333-70-8; VIII, 100333-71-9; IV, 100333-72-0; $Na^+[(Me_3Si)_2C_2B_4H_5]^-$, 91633-70-4; $Na^+[(Me_3Si)(Me)C_2B_4H_5]^-$, 91633-71-5; $Na^+[(Me_3Si)C_2B_4H_6]^-$, 91633-72-6; $SnCl_2$, 7772-99-8.

Supplementary Material Available: Tables of anisotropic temperature factors and isotropic temperature factors for hydrogen atoms of III, listings of structure factors of III and IV (Tables S1–S3), and listings of mass spectrometric data (Table S4) and FT-IR absorptions (Table S5) of IV, V, and VI (21 pages). Ordering information is given on any current masthead page.